JOURNAL OF AEROSOL MEDICINE AND PULMONARY DRUG DELIVERY
Volume 24, Number 1, 2011

Pp. 49–60
DOI: 10.1089/jamp.2010.0843

The Use of Combined Single Photon Emission Computed Tomography and X-ray Computed Tomography to Assess the Fate of Inhaled Aerosol

John Fleming, Ph.D.,[1] Joy Conway, Ph.D.,[2] Caroline Majoral, Ph.D.,[3] Livia Tossici-Bolt, Ph.D.,[1] Ira Katz, Ph.D.,[3,4] Georges Caillibotte, Ph.D.,[3] Diane Perchet, Ph.D.,[3] Marine Pichelin, Ph.D.,[3] Bernhard Muellinger, Dipl. Ing. (FH),[5] Ted Martonen, Ph.D.,[6,7] Philipp Kroneberg, Dipl. Ing. (FH),[5] and Gabriela Apiou-Sbirlea, Ph.D.[8]

Abstract

Background: Gamma camera imaging is widely used to assess pulmonary aerosol deposition. Conventional planar imaging provides limited information on its regional distribution. In this study, single photon emission computed tomography (SPECT) was used to describe deposition in three dimensions (3D) and combined with X-ray computed tomography (CT) to relate this to lung anatomy. Its performance was compared to planar imaging.
Methods: Ten SPECT/CT studies were performed on five healthy subjects following carefully controlled inhalation of radioaerosol from a nebulizer, using a variety of inhalation regimes. The 3D spatial distribution was assessed using a central-to-peripheral ratio (C/P) normalized to lung volume and for the right lung was compared to planar C/P analysis. The deposition by airway generation was calculated for each lung and the conducting airways deposition fraction compared to 24-h clearance.
Results: The 3D normalized C/P ratio correlated more closely with 24-h clearance than the 2D ratio for the right lung [coefficient of variation (COV), 9% compared to 15% $p < 0.05$]. Analysis of regional distribution was possible for both lungs in 3D but not in 2D due to overlap of the stomach on the left lung. The mean conducting airways deposition fraction from SPECT for both lungs was not significantly different from 24-h clearance (COV 18%). Both spatial and generational measures of central deposition were significantly higher for the left than for the right lung.
Conclusions: Combined SPECT/CT enabled improved analysis of aerosol deposition from gamma camera imaging compared to planar imaging. 3D radionuclide imaging combined with anatomical information from CT and computer analysis is a useful approach for applications requiring regional information on deposition.

Key words: aerosol deposition, SPECT/CT imaging

Introduction

Delivery of drugs by inhalation is widely used to treat lung disorders and is also a convenient means of administering drugs systemically to treat diseases in other parts of the body. Knowledge of the fate of drugs in the airways tree is important in optimizing this form of therapy. Information on the deposition of aerosols in the lung has been obtained

[1]Department of Medical Physics and Bioengineering, Southampton University Hospitals, NHS Trust, Southampton, United Kingdom.
[2]School of Health Sciences, University of Southampton, Southampton, United Kingdom.
[3]Medical Gases Group, Air Liquide Centre de Recherche Claude-Delorme, Les Loges-en-Josas, France.
[4]Department of Mechanical Engineering, Lafayette College, Easton, Pennsylvania.
[5]Activaero GmbH, Gemünden, Germany.
[6]CyberMedicine, Laguna Beach, California.
[7]Department of Medicine, University of North Carolina–Chapel Hill, Chapel Hill, North Carolina.
[8]Biomedical Research Institute Mondor (INSERUM, UMR 955), University Paris Est, Créteil, France.

using radionuclide imaging. Two-dimensional (2D) imaging using a gamma camera is the common technique[1] and has been shown to provide reliable measurements of the total deposition in the lungs. Over recent years three-dimensional (3D) radionuclide imaging has also been applied and demonstrated an improved ability to describe the distribution of deposition within the airway tree.[2] Both single photon emission tomography (SPECT) and positron emission tomography (PET) have been used.

SPECT produces a 3D description of the distribution of a gamma-emitting radionuclide in the body using the data obtained from a rotating gamma camera. Both the formation and interpretation of SPECT images are improved with the addition of anatomical image data. To obtain images that are an accurate reflection of the distribution of radioactivity in the body, the counts detected by the gamma camera have to be corrected for attenuation by the body. Different body tissues have different attenuating properties, and anatomical data allows attenuation correction to be performed and quantitative images to be created. Definition of accurate lung outlines also helps to interpret the aerosol deposition data more precisely. In the past, anatomical image data have been obtained from computed tomography (CT)[3] or magnetic resonance imaging (MRI)[4] acquired on separate machines from the SPECT scanner. The SPECT and anatomical images then had to be transferred a common analysis computer and aligned accurately to each other to enable their combined use. Over the last few years combined SPECT-CT scanners have become available that enable SPECT and CT scans to be obtained on the same machine without moving the patient and thus improving the alignment.[5]

This study describes the application of SPECT-CT scanning to the task of quantifying the fate of inhaled aerosols within the body in a pilot *in vivo* study on healthy control subjects. This purpose of the main clinical study is to compare experimental measurements of aerosol deposition from imaging with results of computer modeling. The current article is using the pilot data to illustrate the application of SPECT-CT technology to aerosol deposition measurements. The methodology is described and the results obtained compared with conventional planar imaging analysis.

Methods

Subjects

The pilot study involved five evaluable healthy never-smoker male subjects, between 18 and 65 years old, with no evidence of respiratory disease, and lung function tests within the normal range. This included being free from the common cold and rhinitis for at least 4 weeks before entry into the study. The study was approved by the local ethics committee and the Administration of Radioactive Substances Advisory Committee, and patients gave written consent to participate in it.

Aerosol administration

The radiopharmaceutical aerosol consisted of nebulized aqueous droplets produced from a suspension of Tc-99m labeled millimicrospheres of human serum albumin. It was a commercially available radiopharmaceutical kit, Nanocoll® (GE Healthcare, Piscataway, NJ, USA). The radioaerosol was administered to the subject using either the AKITA$^{2®}$ APIXNEB (for air) or AKITA$^{2®}$ Oxhel device (for Helium Oxygen) (Activaero GmbH, Germany). The AKITA$^{2®}$ device was specially designed to control the ventilatory regime and aerosol characteristics. The Oxhel is the version of the device specially designed to be used with helium/oxygen mixture. It was connected to a vibrating mesh aerosol generator that uses TouchSpray® Technology (Pari Pharma, Germany) capable of delivering an aerosol that has a relatively narrow particle size distribution.

Four variables were taken into consideration:

1. Carrier gas: air or helium/oxygen (78:22% by volume) mixture.
2. Ventilatory regimes: slow ($9\,min^{-1}$) with inspiratory volume of 1000 mL or fast ($15\,min^{-1}$) with inspiratory volume of 600 mL.
3. Aerosol characteristics: small [mass median aerodynamic diameter (MMAD) 3.1 μm, Geometric Standard Deviation (GSD) 1.5] or large (MMAD 5.7 μm, GSD 1.6) particle size distributions.
4. Posture: supine or erect.

Each subject underwent two experiments, the first experiment (A) varying from the second one (B) by one or two variables. The purpose of this pilot experiment was to test the different modes of aerosol delivery and demonstrate the application of SPECT-CT technology.

The first subject underwent the two following experiments: (A) air, slow, large; (B) air, fast, small.

The second subject underwent the two following experiments: (A) air, fast, large; (B) air, slow, small.

The third subject underwent the same experiments as the second in order to study intersubject variability: (A) air, fast, large; (B) air, slow, small.

The fourth subject inhaled a mixture of helium and oxygen: (A) He/O_2, fast, large; (B) He/O_2, slow, small.

The fifth subject inhaled once supine and once erect in order to study the influence of lung position (usual inhalations are performed erect while images are acquired supine): (A) erect, air, fast, large; (B) supine, air, fast, large.

Details of the subjects and the mode of inhalation on each occasion that they were studied are summarized in Table 1.

Image acquisition

Immediately following aerosol inhalation, the subject was instructed to lie down supine on the couch of a GE Infinia dual head gamma camera with CT attachment (GE Medical Systems, Milwaukee, WI, USA). The couch was positioned so that the oropharynx was approximately in the center of the field of view and a 60-sec anterior/posterior planar image pair was acquired. The couch was then moved so that all the lungs and stomach were included in the field of view and a further 60-sec anterior/posterior acquisition was performed. All images were acquired in two windows, the 20% 140 keV Tc-99m photopeak and an 8% scatter window centred on 120 keV. This captured the initial deposition of the aerosol. Without moving the subject, a SPECT acquisition was acquired using 60 projection images each of 20 sec (a total imaging time of 10 min). This was followed by a CT image, which provided 90 slices with an interslice separation of

Table 1. Details of the Five Subjects Studied, the Inhalation Regimes, and the Aerosol Characteristic Used for Each Occasion on Which They Were Imaged

Subject	*Study*	*FRC liter*	*Inhaled volume*	*Rate of inhalation (breaths/min)*	*Posture for inhalation*	*Mass median aerodynamic particle size (micron)*	*Carrier gas*
1	A	3080	1000	9	Erect	5.7	Air
	B	3080	600	15	Erect	3.1	Air
2	A	3170	600	15	Erect	5.7	Air
	B	3170	1000	9	Erect	3.1	Air
3	A	3370	600	15	Erect	5.7	Air
	B	3370	1000	9	Erect	3.1	Air
4	A	3343	600	15	Erect	5.7	Helium oxygen
	B	3343	1000	9	Erect	3.1	Helium oxygen
5	A	2800	600	15	Erect	5.7	Air
	B	1980	600	15	Supine	5.7	Air

4.42 mm. This image took approximately 4 min to acquire and therefore provided a CT image of the thorax at mean tidal breathing. A further SPECT CT image of the oropharynx region was then obtained. The SPECT acquisition was 10-sec per frame. The bed was repositioned to view the lungs and stomach and the planar imaging protocol repeated. This enabled an estimate of the rate of lung clearance, which could be used to correct activities derived from the SPECT image for this factor. Planar imaging of the nebulizer, the exhalation filter, and the standard was also performed. The following day a 24-h planar anterior/posterior image pair of the lungs was acquired with an acquisition time of 300 sec.

The mean effective radiation dose received by the subjects was 1.1 mSv, 0.3 mSv from the radionuclide, and 0.8 mSv from the low dose CT scan.

Reconstruction

The SPECT images were reconstructed on a Xeleris workstation (GE Medical Systems). The reconstruction was performed using Ordered Subsets Expectation Maximization (OSEM) with a postreconstruction smooth using a 3D Butterworth filter with a cutoff of 0.5 cycles/cm. The algorithm included scatter correction using the scatter energy window method and attenuation correction using an attenuation map derived from the CT scan. All images were transferred to a Unix workstation for processing with the Portable Image Computer Software (PICS) system.[6]

Definition of volumes of interest

The first part of the processing was to outline the following regions: trachea and main bronchi, right lung and left lung. The CT images were first converted to a dataset with cubic voxels of 4.42 mm. Segmentation was then carried out semiautomatically using a threshold based, volume-growing algorithm, with a start point defined visually in the trachea. Separation of each lung from the bronchi was achieved using positions of the right and left hila, again defined manually from visual display of the transaxial and coronal images. The hila were defined as the first bifurcation points of the main bronchi.

Planar analysis

The initial distribution of aerosol within the body was determined as described in detail in a previous publication[7] and the method is outlined here. Geometric mean images were formed for both the lung and oropharynx areas. Regions were then defined over the following organs: right lung, left lung, stomach, trachea, and bronchi and oropharynx. The right and left lung regions were defined automatically using a 10% contour on a simulated lung volume image.[7,8] This was created by defining a uniform 3D distribution of activity in a computer model of the airway tree and simulating the corresponding gamma camera image using the attenuation map derived from the CT scan to model the effect of tissue attenuation.[8] The other regions were defined manually from a visual display of the initial aerosol deposition image. Attenuation correction factors for each region were calculated from thickness measurements obtained automatically from the CT images. The counts were corrected for background using a region of interest toward the edge of the images, for attenuation and for radioactive decay. They were then converted to megabecquerels (MBq) using a gamma camera sensitivity measurement obtained from the anterior image of the standard. The activity in the exhalation filter and that remaining in the nebulizer were calculated from the counts in the respective anterior images.

The amount leaving the nebulizer was calculated in two ways: (1) as the difference between the activity initially placed in the nebulizer and that left after inhalation, I_1, and (2) as the sum of all the activities accounted for in the body and exhalation filter, I_2. The comparison between I_1 and I_2 gave a measure of dose accountability in the measurements. The activities in each organ were expressed as percentages of I_2.

SPECT analysis. The SPECT images were first subjected to smoothing of each transaxial slice with two passes of a standard 4-2-1 smoothing operator. This was to make the resolution of the images compatible with that assumed in the partial volume correction algorithm described below. A description of the spatial distribution of the aerosol deposition from center to periphery of the lungs was then obtained by

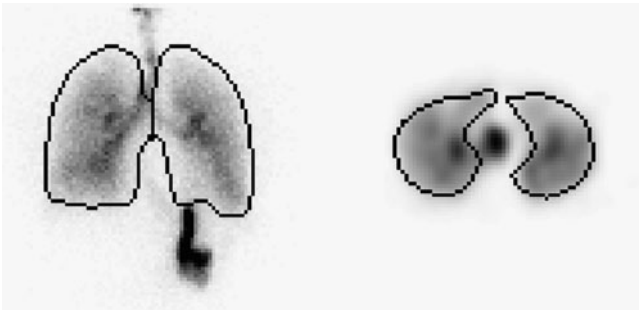

FIG. 1. Example images demonstrating the inclusion of activity in the bronchi and part of the trachea in the 2D regions representing the lung. The left image shows an anterior planar gamma camera view of the lungs with the lung regions overlaid. The right image depicts a transverse section of the SPECT dataset with lung regions overlaid. Activity in the trachea is clearly separate from the lung regions.

dividing each lung volume into 30 concentric shells based on the fractional distance from the hilum to the periphery of the lung.[3] The count in each shell was computed, S_i. The relatively poor resolution of the SPECT images meant that some of the counts in a particular shell appeared in the image in an adjacent shell or in the case of peripheral shells outside the lung volume altogether. This partial volume effect was corrected using knowledge of the crosstalk between shells derived from simulated data. The technique was based on a previously described method[9] with the modification that the technique of maximum likelihood expectation maximization (MLEM)[10] was used in place of the arithmetic reconstruction technique (ART). The count in each shell after partial volume correction, CS_i, was calculated.

One of the potential advantages of SPECT is in giving more precise measurement of the division of activity between the trachea and main bronchi and the lungs. In a planar image, the lungs regions obtained from an isocontour of the volume or ventilation image often include a good proportion of the trachea and main bronchi. This means that the activity in the lungs will be overestimated, and that the activity in the trachea and main bronchi will be underestimated. Figure 1 shows an example where the lung regions of interest on the planar image clearly include all the main bronchi and some of the trachea.

The total activity within each lung was evaluated from SPECT by summing the count rate in the partial volume corrected shell data. This was then divided by the sensitivity of the SPECT images in counts per second per MBq derived from a phantom study to obtain the activity in MBq. The activity in the trachea and main bronchi were evaluated from the counts in the corresponding volume of interest derived from the CT scan. To correct for the partial volume effect, the volume of interest (VOI) was dilated by 13 mm. Dilation in any particular direction was stopped when the volume would have expanded into either lung volume. The activity was derived from the count rate in this dilated volume divided by the SPECT sensitivity.

The activities in the lungs and TB volumes obtained from SPECT were compared to those obtained by planar imaging. To do this accurately, it was necessary to correct for the mucociliary clearance that was taking place during the SPECT study. The mucociliary clearance rate was measured by comparing the counts in the lungs and TB regions in the planar images before and after SPECT. Assuming a linear change in activity over this period, the counts in the SPECT image were corrected to the inhalation time.

Quantification of the regional distribution of deposition

In conventional planar scintigraphy, a measure of regional distribution of aerosol is obtained by dividing up the region of interest representing the lung into central and peripheral regions. On the basis that airways branch approximately radially from the hilum to the periphery of the lung, this enables a crude estimate of the distribution of aerosol between central conducting airways and peripheral alveolated airways. One important drawback of this analysis is that the aerosol in the central region is mainly in alveolated airways and so at best an index of conducting airway deposition can be obtained. The 3D data from SPECT provided by the shell analysis allows a more precise quantification of the spatial distribution of aerosol and the partial volume correction improves the accuracy.

The spatial distribution of deposition was summarized by the central-to-peripheral ratio (C/P). In this study this was calculated from both 2D and 3D C/P deposition ratios. The 2D C/P ratio (C/P_{2D}) was calculated for the right lung only by performing a 2D shell analysis.[11] The lung region of interest (ROI) was divided up into 10 concentric annuli and applied to the attenuation corrected geometric mean image. The 2D ratio was calculated by dividing the activity in the central five shells by that in the outer five

$$C/P_{2D} = \frac{\sum_{i=1}^{5} PS_i}{\sum_{i=6}^{10} PS_i}$$

where PS_i is the count in shell i on the planar image. This analysis was only performed for the right lung, as overlap of counts from the stomach can invalidate results from the left lung. As the C/P ratio has been shown to depend on lung shape,[12] the value was normalized to the 2D C/P ratio of the simulated volume image, also corrected for attenuation using the attenuation map derived from CT. The normalized 2D C/P ratio, nC/P_{2D} was:

$$nC/P_{2D} = \frac{C/P_{2D} \textit{ of the initial planar image}}{C/P_{2D} \textit{ of the volume image}}$$

An analogous normalized 3D C/P ratio was calculated by summing the partial volume corrected activity in both the inner and outer 15 of the 30 3D shells and calculating the ratio C/P_{3D}. This was divided by the corresponding ratio for the simulated 3D volume image, to give the normalized ratio, nC/P_{3D}. The 3D ratios were calculated for both left and right lungs.

Despite the improvements in the spatial description of deposition available from 3D imaging, the data still only provide an approximation to deposition in the airway tree. This is because shell numbers do not relate directly to generation numbers. However, a conceptual model of the spatial arrangement of the lung airway is available that describes

the volume (v_{ij}) of each shell, i, in each generation, j,[13] This enables an equation to be described relating the unknown deposition concentration per unit air volume in each generation g_j to the measured deposition per shell after correction for the partial volume effect CS_i

$$CS_i = \sum_{j=1}^{\text{maxgen}} g_j \cdot V_{ij} \quad (1)$$

This equation can be solved for the deposition concentration per generation g_j. The upper limit of integration, maxgen, is the maximum generation penetrated by the aerosol. This is calculated from the inspired volume, TV, expressed as a fraction of the total lung volume at the end of inspiration (F), that is,

$$F = \text{TV}/(\text{FRC} + \text{TV})$$

where FRC is the functional residual capacity. F is converted to a fractional generation number by comparing its value to a table of fractional cumulated generation volumes C_j.

$$C_j = \frac{\sum_{k=2}^{j} V_k}{\sum_{k=2}^{23} V_k}$$

where V_k is the total volume of each generation.

$$V_k = \sum_{i=1}^{30} V_{ij}$$

The value of F will fall between two discrete generation numbers j_p and j_{p+1}. The precise value of fractional generation penetration is then obtained by interpolation between these generations, that is,

$$\text{maxgen} = j_p + \frac{(F - C_{j_p})}{(C_{j_{p+1}} - C_{j_p})}$$

Equation 1 was solved using the MLEM technique.[10] The total deposition per generation, G_j, was calculated by multiplying the concentration by the air volume per generation, V_j.

This estimated deposition per generation data was then summarized by calculating four parameters, the bronchial airways deposition fraction, badf, (generations 2–8), the bronchiolar airways deposition fraction, bbdf (generations 9–15), the conducting airways deposition fraction based on the ICRP definition of conducting airways in the lung (generations 2–15), cadf,[14] and the conducting airway deposition fraction based on the Weibel definition of conducting airways, wdf.

$$wdf = \frac{\sum_{j=2}^{16} G_j + 0.88 \cdot G_{17} + 0.75 \cdot G_{18} + 0.5 \cdot G_{19}}{\sum_{j=2}^{23} G_j} \quad (2)$$

Weibel estimated that a fraction of the airways in generations 16–19 were part of the conducting airways.[15]

Left lung versus right lung deposition

The parameters defined above describe the distribution of the activity in the left and right lung as fractions of deposition in each individual lung. It is also possible to describe the distribution relative to the total deposition in both lungs. This allows the left and right deposition to be compared in absolute terms. The central spatial deposition in 3D for the right lung as a fraction of total lung activity (the right central to total lung spatial deposition fraction, $\text{csdft}_{3\text{Dr}}$) is given by

$$csdft_{3Dr} = \frac{\sum_{i=1}^{15} SSR_i}{RLA + LLA}$$

where SSR_i is the SPECT shell data for the right lung and RLA and LLA are the total lung activities for the left and right lungs, respectively.

Similarly, we can describe the airways deposition fractions in terms of total lung activity. For example, the bronchial airways fraction for the right lung as a fraction of the total lung activity (the right bronchial airways to total lung deposition fraction, badft_r) is given by

$$badft_r = \frac{\sum_{j=2}^{8} G_{rj}}{RLA + LLA}$$

where G_{rj} is the deposition in generation j for the right lung. These parameters allow comparison of the fractional regional deposition in the left and right lungs relative to a common total.

The left-to-right ratios for each of the above spatial and airways parameters were also normalized to the left-to-right ratio of lung volume.

Statistical analysis

Systematic differences between mean values were determined by the Student's t-test. A p-value inferior to 0.05 was considered as a significant difference. Random variation between two variables was obtained after linear regression either as the standard error of the estimate or the coefficient of variation. Differences between standard errors were determined by the F test. Statistical analysis was performed using Microsoft Excel.

Results

The total deposition in each lung for planar and SPECT imaging is shown in Figure 2. The mean reduction in counts due to mucociliary clearance during the SPECT imaging was estimated to be 2.3%. After correction for this effect the planar values (pre-SPECT images) were systematically higher than the SPECT by 11.5%. The random difference between these two measurements as determined by the coefficient of variation is 4.4%.

The results of dose accountability are shown in Figure 3. Note that these results used planar imaging assessment of organ activity. The mean total activity leaving the nebulizer for the first measurement obtained as the difference between the activity put in the nebulizer and that left after inhalation was 74.1 ± 20.7 MBq. The second measurement obtained by

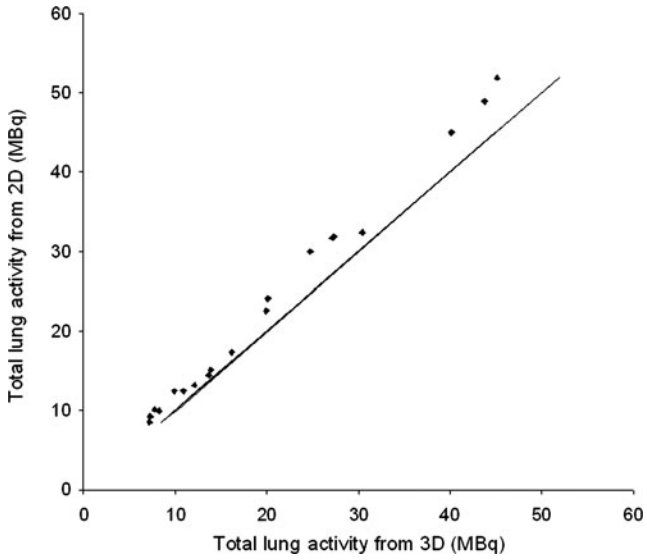

FIG. 2. The total deposition in each lung determined from planar and SPECT imaging.

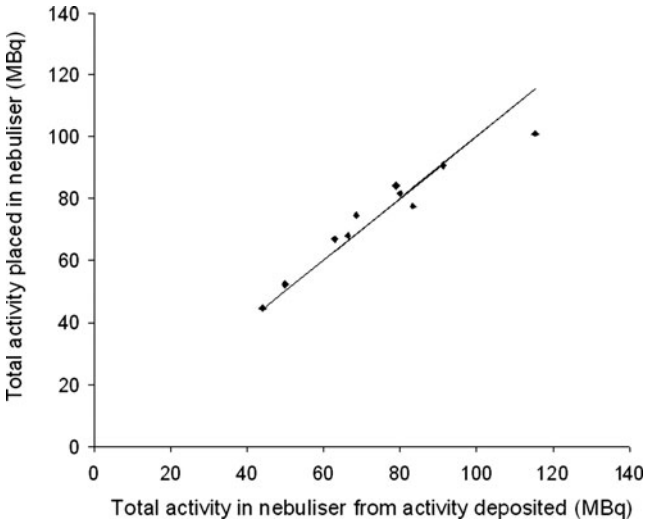

FIG. 3. The total activity leaving the nebulizer assessed from (1) the difference in activity put into the nebulizer and that left after inhalation and (2) the sum of the activity accounted for in the body and exhalation filter.

summing the activity in the body and exhalation filter gave a mean value of 74.2 ± 17.1 MBq. The Student's *t*-test gave a *p*-value of 0.99, meaning that there was no significant systematic difference between the two measurements. The random difference as measured by the coefficient of variation was 8%. In order to investigate the suggestion that the true attenuation correction factor depends strongly on C/P ratio,[15] the percentage difference in activity measured by the gamma camera from that put into the nebulizer was plotted against the normalized 3D C/P ratio. No significant correlation was observed. The mean attenuation correction factor (ACF) for the lung found in this study was 2.16 ± 0.10 (1 SD).

The distribution of inhaled aerosol between different organs is shown in Table 2. These results were also based on planar image data. The values shown are expressed as a percentage of the total inhaled. In all four subjects who inhaled the 3.1 μm particle on one occasion and the 5.7 μm particle on the second, the deposition in the thoracic airways was higher for the small particle and the deposition in the extrathoracic airways higher for the larger particle. Subject 4 had the same inhalation protocol as subjects 2 and 3 except that helium–oxygen was used as the carrier gas instead of air. Although conclusions cannot be drawn from one subject it was noted that there was less thoracic deposition for the helium oxygen inhalation and more exhaled. In subject 5, who was imaged erect and supine on the two occasions using the same inhalation protocol, there was more extrathoracic deposition and less in the thorax when supine.

The parameters of both spatial and generational estimates of pulmonary regional deposition are shown in Table 3. All values are expressed as fractions of the total deposition in the lung. In all subjects who inhaled the small particle on one occasion and the large particle on the other, the pattern of results pointed to a larger fraction of deposition in the central airways for the larger particles. In subject 4, who inhaled the helium–oxygen mixture, some regional parameters suggest a lower deposition in the central airways compared to the use of air in subjects 2 and 3. In subject 5, all regional parameters suggested a more central deposition obtained in the erect position compared to supine.

The correlation between the 2D and 3D normalized C/P ratio is shown in Figure 4. Data is only presented for the right lung, as it was not possible to reliably estimate the left lung, due to the overlay of the stomach. There is a highly significant

Table 2. The Distribution of the Inhaled Aerosol in Different Lung Regions as a Percentage of the Total Inhaled

Subject	*Study*	*Right lung %*	*Left lung %*	*Trachea/bronchus %*	*Total thoracic %*	*Extrathoracic %*	*Exhaled %*
1	A	44.6	30.5	6.0	81.2	15.6	3.2
	B	53.8	31.5	3.1	88.3	3.5	8.2
2	A	43.1	32.8	4.9	80.7	16.8	2.5
	B	51.5	37.0	1.6	90.0	5.4	4.6
3	A	45.2	41.1	3.2	89.6	7.5	3.0
	B	46.2	43.5	2.7	92.4	3.2	4.4
4	A	40.0	37.7	5.2	82.9	14.3	2.8
	B	41.5	41.2	1.7	84.4	2.6	13.0
5	A	35.8	29.5	4.3	69.6	24.1	6.4
	B	28.4	23.6	2.5	54.4	42.8	2.8

Table 3. Estimates of Pulmonary Regional Deposition in Each Lung

Subject	Study	Lung	2D normalized C/P ratio	3D normalized C/P ratio	Bronchial airways deposition fraction	Bronchiolar airways deposition fraction	Weibel conducting airways deposition fraction	24-h clearance
1	A	R	2.02	2.97	0.24	0.17	0.51	0.65
		L		3.96	0.35	0.19	0.72	0.64
	B	R	0.94	1.07	0.02	0.09	0.35	0.37
		L		0.83	0.02	0.10	0.36	0.37
2	A	R	1.11	1.91	0.12	0.09	0.44	0.47
		L		2.65	0.18	0.10	0.49	0.49
	B	R	0.87	0.81	0.01	0.06	0.24	0.32
		L		0.92	0.03	0.06	0.26	0.31
3	A	R	1.21	1.94	0.19	0.21	0.73	0.47
		L		2.33	0.19	0.21	0.72	0.50
	B	R	1.07	1.14	0.03	0.07	0.26	0.27
		L		1.36	0.03	0.06	0.26	0.28
4	A	R	1.14	1.55	0.08	0.14	0.59	0.43
		L		2.20	0.13	0.14	0.63	0.44
	B	R	0.85	0.68	0.01	0.07	0.29	0.27
		L		0.96	0.02	0.07	0.30	0.29
5	A	R	1.11	1.51	0.04	0.08	0.33	0.45
		L		1.96	0.12	0.16	0.56	0.47
	B	R	1.08	1.29	0.03	0.06	0.26	0.35
		L		1.57	0.07	0.07	0.30	0.38

The 2D normalized central-to-peripheral ratio was only calculated for the right lung due to the problem of overlay of the stomach on the region representing the left lung.

correlation between the two measures, but with the 3D parameter having a considerable extended dynamic range (0.68–2.97) compared to the 2D ratio (0.85–2.02). This is expected due to the reduction in contrast between central and peripheral counts due to the contribution to counts in the central region from activity in peripheral lung tissue.

Measurement of 24-h clearance gives a measure of deposition in the conducting airways. These data correlated well with both 2D and 3D normalized C/P ratio (Fig. 5). The coefficient of variation of empirical estimation of 24-h clearance from the normalized 3D C/P ratio was 12%. For the right lung alone this was 9%. The corresponding value for the right lung from 2D normalized C/P ratio was significantly higher at 15% ($p < 0.05$).

The comparison of 24-h clearance with the estimated deposition in the conducting airways using the analysis of the SPECT data is shown in Figure 6a and b. Data are presented for each lung separately. Figure 6a shows the results assuming the standard International Commission on Radiological Protection (ICRP) definition of the conducting airways in the lung represented by generations 2–15. Figure 6b shows the results obtained by assuming the Weibel definition of the extent of the conducting airways described above in Equation 2. Using the ICRP definition of the conducting airways the 24-h clearance was always higher than the conducting airways deposition fraction. This suggests that aerosol was being cleared from airways beyond

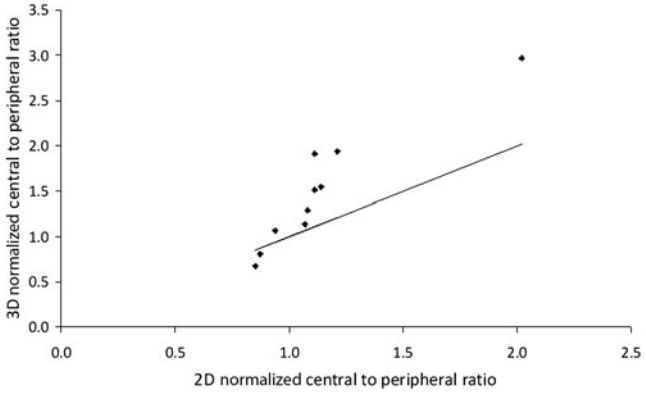

FIG. 4. The variation of 3D normalized central-to-peripheral ratio with the corresponding 2D ratio. The line is the line of identity.

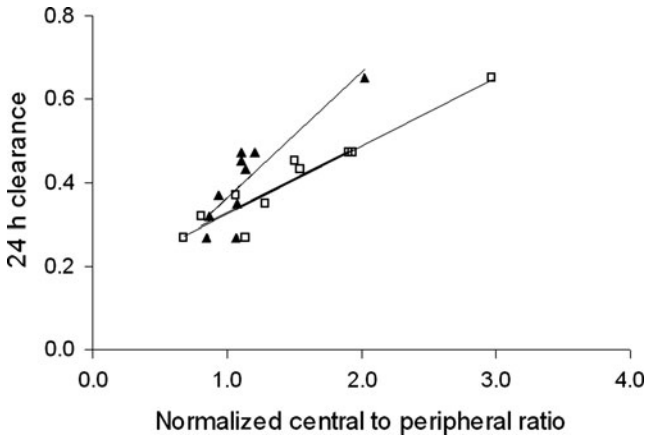

FIG. 5. The variation of 24-h clearance for the right lung with (**a**) 2D normalized central to peripheral ratio (▲) and (b) 3D normalized central-to-peripheral ratio (□). The lines are the lines of least squares linear regression.

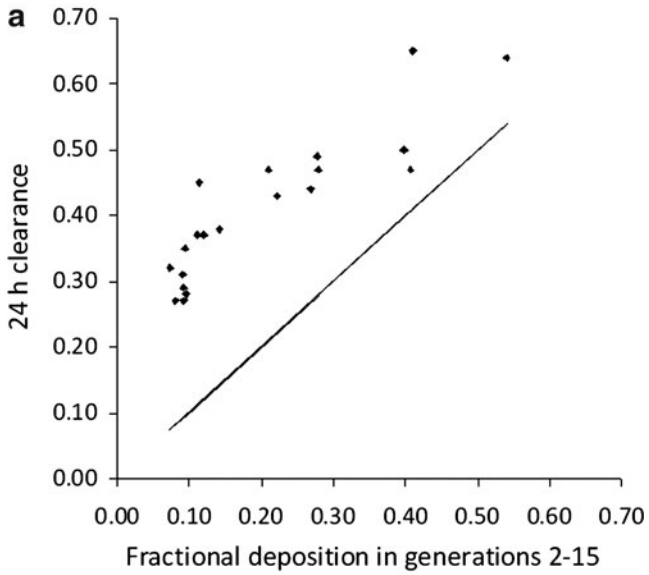

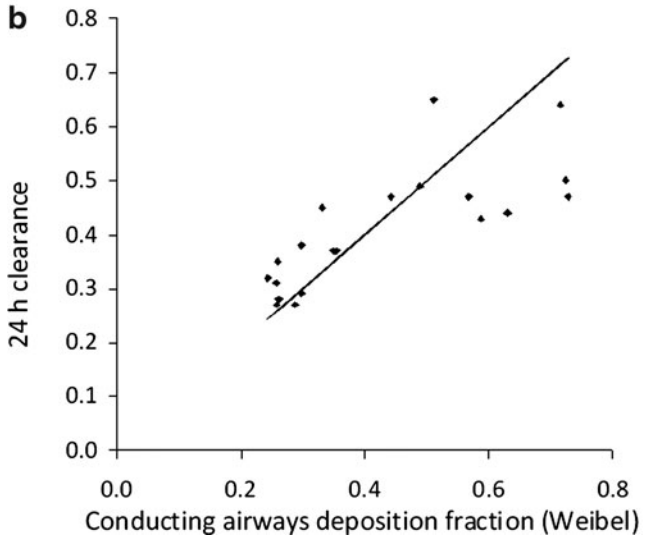

FIG. 6. (**a**) The variation of 24-h clearance with the estimated fractional deposition in generations 2–15. The line is the line of identity. (**b**) The variation of 24-h clearance with conducting airways deposition fraction assuming the definition of the conducting airways in the Weibel Model. The line is the line of identity.

generation 15. This is indeed consistent with Weibel's observation that a fraction of generations 16–19 are conducting airways. Using his definition of conducting airways, there was no significant difference between the mean 24-h clearance and the mean Weibel conducting airways deposition fraction. However, the correlation was significantly different from the line of identity; at lower values of wdf the 24-h clearance was higher and at higher values it was lower. The coefficient of variation of estimating 24-h clearance was 18%. This was significantly higher than that obtained using the 3D normalized C/P ratio ($p < 0.05$).

The comparison of deposition in the right and left lungs is shown in Figure 7. The total activity deposited is significantly higher in the right lung than in left lung ($p < 0.005$). The left-to-right ratio was 0.82 ± 0.14 (1 SEM). This is expected due to the larger volume of the right lung compared to the left. The left-to-right ratio for total lung volume obtained from CT was 0.83 ± 0.14 (1 SEM), which was not significantly different. The percentage aerosol in the right lung correlated significantly with the percentage lung volume ($p < 0.005$). The standard error of the difference was 2.0 percentage points. When normalized to lung volume, the left-to-right ratio for deposition was 0.98 ± 0.02.

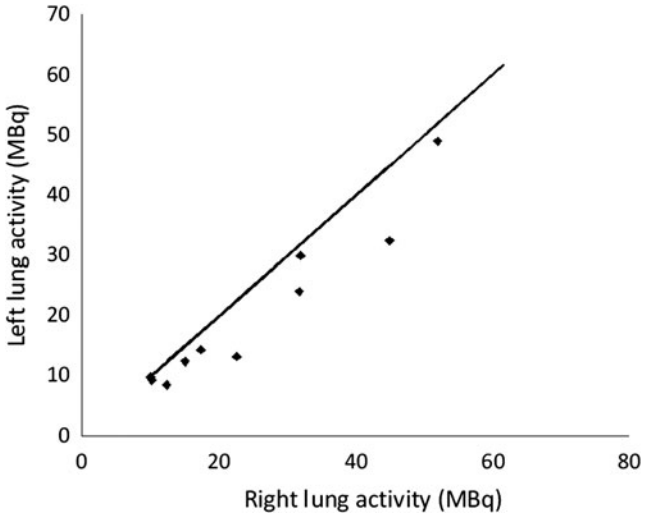

FIG. 7. Comparison of total deposition in the right and left lungs. The line is the line of identity.

The results on the left-to-right ratios of the parameters describing regional deposition are shown in Table 4. The comparison of the normalized 3D C/P ratio for the left and right lungs is shown in Figure 8. The left-to-right ratio was 1.24 ± 0.06 (1 SEM), which was significantly different from one ($p < 0.005$). The degree of difference was significantly correlated to the C/P ratio ($p < 0.005$). The bronchial airways deposition fraction was also significantly higher for the left lung ($p < 0.001$) (Fig. 9) . The mean value of 1.79 was significantly higher than for the normalized 3D C/P ratio ($p < 0.01$).

When the regional deposition fractions were calculated relative to total deposition the differences between left and right were lower. The left-to-right ratio for the central to total lung spatial deposition fraction was not significantly different from one. However, the corresponding value for bronchial airways deposition was 1.47 ± 0.20 1 SEM ($p < 0.01$), showing that even in absolute terms the central deposition was higher in the bronchial airways of the left lung. When these data are expressed as fractions of total lung deposition and normalized for lung volume, the left-to-right ratios for both central spatial and bronchial airways deposition were significantly greater than 1. Again, the ratio is significantly higher for the airways parameter compared to the spatial parameter.

Discussion

The use of combined SPECT-CT scanning clearly has some important advantages over both planar imaging and SPECT scanning using anatomical data obtained from separate scanning devices. In this discussion, we consider both the

Table 4. Left-to-Right Ratios of Parameters Describing the Regional Deposition in the Lung from 3D Analysis

Parameter	*Mean*	*SEM*	*Significance of difference between left and right*
Normalized central-to-peripheral ratio (3D)	1.24	0.06	<0.001
Central to total spatial deposition fraction (3D)	0.97	0.08	NS
Normalized central to total spatial deposition fraction (3D)	1.15	0.07	<0.05
Bronchial airways deposition fraction	1.79	0.24	<0.001
Bronchial airways to total lung deposition fraction	1.47	0.20	0.01
Normalized bronchial airways to total lung deposition fraction	1.79	0.26	0.001

specific results of the study described here, and also the broader aspects of comparison between the imaging methods for determining aerosol deposition.

The ability of planar imaging to measure total deposition in the lung has come under particular scrutiny in the literature.[16,17] It was therefore felt important to include a clear validation of the planar analysis of this study. This was done in two ways: (1) using the dose accountability experiment in which the total activity leaving the nebulizer measured using an isotope calibrator was compared to that obtained from gamma camera imaging, and (2) by comparing total lung activity measurements from planar imaging with those from SPECT.

There was no systematic difference between the two measurements of total activity leaving the nebulizer, and the root mean square difference was 8%. The gamma camera assessment of activity in this measurement relied solely on planar imaging, and therefore the results confirmed that the planar quantification methods used were working successfully. This included the assessment of lung activity using global attenuation correction factors derived from total thickness measurements of the thorax. The mean ACF for the lung was 2.16. This confirmed previous estimates of ACF of around 2 from several different sources.[7,12,18] There was no correlation between dose accountability and C/P ratio, suggesting that these global ACFs worked equally well for uniform distributions of aerosol and those with a high central deposition. We could therefore find no evidence advocating for the use of a high ACF in central deposition patterns as suggested by Moller et al.[16] The findings in this study concur with a recent analysis of the regional variation of ACF derived from CT scans.[19] This indicated that the ACF for central and peripheral regions was very similar.

The total activity in the lung derived from SPECT correlated well with that derived from planar imaging. The process of mucociliary clearance was relatively slow compared to the imaging period. The mean correction in activity was just 2.3%. After correction the SPECT value was systematically lower than the planar values by 11.5%. This could mean that planar values of lung activity were overestimated either due to some systematic error in the derivation of the ACFs or to the inclusion of activity in the trachea and bronchi in the lung regions of interest. Alternatively, there could be an underestimation in the SPECT values. Phantom studies of the GE Infinia camera have suggested that the algorithm used for SPECT reconstruction may result in underestimation of activity concentration with the degree of underestimation dependent on the total attenuation in the object (J. McDonald, personal communication, 2008). Therefore the value for SPECT sensitivity obtained in a particular phantom, as used in this study, may not apply exactly, due to intersubject variation in attenuation. It should be noted,

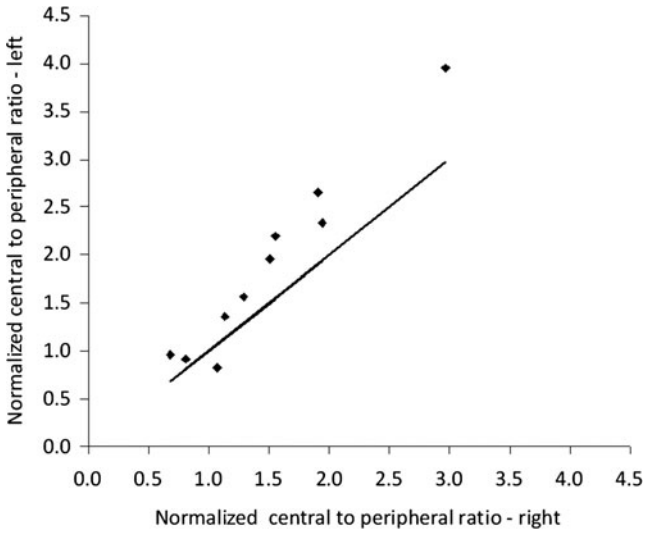

FIG. 8. Comparison of the 3D normalized central-to-peripheral ratio in the right and left lungs. The line is the line of identity.

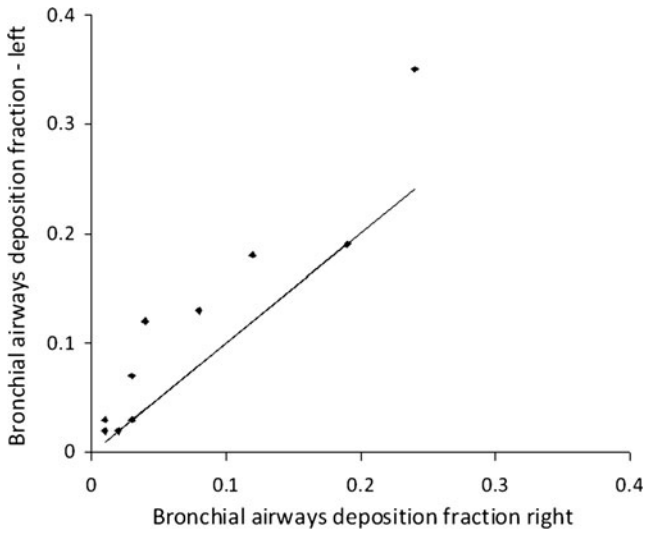

FIG. 9. Comparison of the bronchial airways deposition fraction in the left and right lungs.

however, that this difference in activity values was relatively small, and also applied to the absolute assessment of activity. Because the difference was systematic, the fractions of total-body deposition in each organ derived from SPECT differed by only a few percent from those obtained from planar imaging.

Surprisingly, the activity in the trachea and main bronchi from planar imaging was 58% higher than that derived from SPECT. It had been expected that planar estimates might be lower due to parts of the trachea and main bronchus not being included in the ROI. The most probable explanation for the overestimate is the contribution of scattered radiation from lung activity into this region. Previous studies have shown that lung activities derived from planar imaging with and without scatter correction are very similar.[7] However, this may not apply to assessment of activity in the trachea and main bronchus. The scatter contribution from the much higher activity in the adjacent lung structure may make a large contribution to the counts in the region. The estimate from SPECT imaging should be, in theory, considerably more accurate than that from planar imaging.

The differences in deposition measurements obtained with different inhalation regimes generally followed the expected patterns. Use of the larger 5.7-μm particles compared to the 3.1-μm particles gave rise to higher deposition in the extrathoracic and central lung airways and less exhaled, all findings expected from previous measurements and computer modeling.[14] The low amounts of aerosol exhaled are consistent with estimates from previous imaging studies.[20] However, this is at variance with modeling estimates, which tend to predict a much higher exhaled fraction particularly for particles of around 2 μm diameter.[21] The use of helium as the carrier gas in the one subject studied generally gave similar deposition results compared to air. However, there was relatively higher penetration of aerosol to the lung periphery and more exhaled compared to the two subjects given the same aerosol inhalation regime with air.

The 24-h clearance measurement in control subjects is expected to give an estimate of the deposition in the conducting airways. It therefore provided a means of validating the parameters of regional deposition derived from SPECT imaging. The 3D normalized C/P ratio showed a very good correlation with 24-h clearance. The correlation was significantly better than that for the 2D C/P ratio ($p < 0.05$). This confirms the value of 3D imaging in providing a more accurate and precise estimate of spatial distribution of deposition in the airways.[9]

The deposition fraction in the conducting airways, cadf (generations 2–15), showed good correlation with the 24-h clearance (Fig. 6a). However, it was systematically lower than the 24-h clearance, which suggests that there are ciliated airways beyond generation 15, as proposed by Weibel.[15] This finding agrees with a previous comparison of SPECT derived airway deposition measurements and 24-h clearance.[21]

When the Weibel definition of the conducting airways is used to calculate the deposition fraction (wdf), the systematic difference with 24 h clearance is much lower (Fig. 6b). This provides encouraging evidence for the validity of the generational parameters derived from SPECT-CT imaging. The correlation is improved compared to the previous study,[21] which might be explained for a number of reasons. (1) The current experiment used precise control of inhalation using the AKITA^2 device. This enabled accurate assessment of the maximum airway generation to which the aerosol was delivered (maxgen), which is an important parameter in the calculations. (2) The estimation of maxgen may also have been improved by using the new equation [TV/(TV + FRC)]. The previous assumption that the fraction of lung volume penetrated by aerosol was IV/FRC did not take into consideration the increase in lung volume during inspiration. (3) The software used to calculate the deposition per generation used in this study has also been improved by using a different stopping criteria compared to that used previously. Simulation studies had shown that the original stopping criterion occasionally allowed the algorithm to overiterate toward an inferior solution. In addition, the use of 30 shells in this study means that information theory requirements of having more equations than unknowns are met. (4) The use of CT data to provide attenuation correction and the lung outline are both potentially more accurate than the use of magnetic resonance imaging (MRI), performed on a different device.

The method of deriving deposition per generation has clearly been improved compared to previous versions. However, the resulting correlation with 24-h clearance was inferior to that with the normalized 3D C/P ratio. This is somewhat disappointing given that the C/P ratio is a relatively crude parameter of regional distribution, which does not take into account the depth of inspiration, which in theory should be a good predictor of 24-h clearance. This may be due to the instabilities in the shell to generation algorithm despite the improvements listed above. It is anticipated that further improvements could be made in this calculation under the general description of individualized lung models. The current version relies on the conceptual model of the lung.[13] This describes the spatial distribution of the different airways relative to the shell model of the lung.[3] Although this has been validated against CT, newer more accurate models are now available. High-resolution CT now allows images of the airway of individual patients up to about generation 6. This has enabled the creation of the hybrid model of the lung that uses real measurements of the early generations supplemented by the conceptual model for the rest of the airway.[22] Attempts to model the rest of the airway tree with the spatial location of actual airways have also been made.[23–25] Use of these improved models should result in a more accurate analysis of deposition from SPECT-CT data.

Use of new models will also require use of improved algorithms for calculating airway deposition. The current method performs the calculation in several stages, dividing the spatial data into shells, performing a correction of the shell data for the partial volume effect and then converting the shell data to a description by generation. Improvements could, in principle, be made by defining the spatial extent of the airway of each generation in each voxel. The calculation of deposition per generation could then be performed directly from data of measured activity per voxel.

SPECT imaging has also allowed comparison of deposition patterns in the right and left lungs. The left lung is often not analyzed in planar measurements due to the overlay of the stomach with the base of the left lung in some subjects. Analysis of SPECT studies uses 3D volumes of interest rather

than 2D regions. These can be perfectly separated using the CT images, although there may be some overlap of counts from the two regions due to breathing motion and the partial volume effect. However, this will generally be much smaller than the overlap of 2D regions and can be corrected using crosstalk correction techniques such as that used to correct the shell data for the partial volume effect.[9]

The finding that the left lung has greater central deposition than the right is consistent with previous results. Studies aiming to target aerosol delivery using bolus techniques have shown that shallow boluses targeted toward the central conducting airways are preferentially deposited in the left lung, whereas those targeted toward the lung periphery are more evenly distributed between left and right lungs.[26,27] The results of our study confirm these findings. The left-to-right ratio of lung volume of 0.83 agrees closely with the 0.85 found for ventilation imaging by Moller et al.[27] The left-to-right ratio for total lung deposition normalized to lung volume was not significantly different to 1, again agreeing with the results of Moller et al. for a deep bolus. The regional parameters confirm that when normalized to lung volume there is significantly greater deposition in central airways in the left than the right lung. The difference obtained using the derived airway parameters was significantly greater than from spatially derived values. When absolute deposition was calculated, only the airways parameters showed a significant difference. The mean value of left-to-right ratio for the bronchial airways to total lung deposition fraction normalized for lung volume of 1.79 was very similar to that found by Moller et al.[27] of 1.85. This gives independent validation of their results.

Moller et al.[27] demonstrate that the increased deposition in the central region of the left lung is related to similarly increased ventilation. The finding in this study that the left-to-right differences appear proportional to C/P ratio is consistent with this explanation. An alternative explanation, however, might be that there is more deposition by gravitational sedimentation in the early airway generations of the left lung due to being more horizontal than those of the right. Further work to elucidate this will be carried out using computer simulation based on the realistic models of the lung obtained from high-resolution CT.

The use of a CT scan to provide anatomical information and allow accurate attenuation correction increases the radiation dose to the patient compared to alternative approaches using magnetic resonance images[4] or transmission imaging.[28] However, the low-dose CT regime used in this study only gives a modest dose to each subject, considerably below annual background radiation levels. This additional radiation burden is considered justified in the light of the better anatomical data provided on the lung outline and hilum positions. Some SPECT/CT scanners use a high-resolution multislice CT device. This would give a higher dose to the subject of about 4 mSv, approximately twice the annual natural background radiation dose. However, this protocol would provide even more anatomical information, in that breathhold CT could be employed, allowing definition of the first few generations of the actual airways. This additional information would give the opportunity for improved analysis of aerosol deposition in relation to anatomy. This will be the subject of further study.

In conclusion, this study has demonstrated the application of SPECT-CT to the assessment of regional deposition of aerosol. The use of combined data has produced estimates of deposition in the airways, which show good consistency with total deposition estimates from planar imaging and regional deposition estimates from 24-h measurements. The use of 3D imaging has facilitated analysis of the left lung and this study has provided independent validation of increased deposition per unit volume in the central airways of the left lung compared to the right.

Acknowledgments

The authors thank Sandra Johns, superintendent radiographer of the Department of Nuclear Medicine of Southampton University Hospitals NHS Trust, and her team for performing the imaging studies. John Fleming and Joy Conway acknowledge the support of the Southampton Respiratory Biomedical Research Unit funded by the U.K. National Institute of Health Research.

Author Disclosure Statement

No conflicts of interest exist.

References

1. Newman SP, Pitcairn G, and Hirst PH: A brief history of gamma scintigraphy J Aerosol Med. 2001;14:139–145.
2. Fleming JS, and Conway JH: Three-dimensional imaging of aerosol distribution. J Aerosol Med. 2001;14:147–153.
3. Perring S, Summers Q, Fleming JS, Nassim MA, and Holgate ST: A new method of quantification of the pulmonary regional distribution of aerosols using combined CT and SPECT and its application to nedocromil sodium administered by metered dose inhaler. Br J Radiol. 1994; 67:46–53.
4. Fleming JS, Halson P, Conway JH, Moore E, Nassim MA, Hashish AH, Bailey AG, Holgate ST, and Martonen TB: Three dimensional description of pulmonary deposition of inhaled aerosol using data from multimodality imaging. J Nucl Med. 1996;37:873–877.
5. Bocher M, Balan A, Krausz Y, Shrem Y, Lonn A, Wilk M, and Chisin R: Gamma camera-mounted anatomical X-ray tomography: technology, system characteristics and first images. Eur J Nucl Med. 2000;27:619–627.
6. Fleming JS, Britten AJ, Perring S, Keen AC, and Howlett PJ: A general software system for the handling of medical images. J Med Eng Technol. 1991;15:162–169.
7. Fleming JS, Conway JH, Bolt L, and Holgate ST: A comparison of planar scintigraphy and SPECT measurement of total lung deposition of inhaled aerosol. J Aerosol Med. 2003;16:9–19.
8. Fleming JS, Hashish AH, Conway JH, Hartley-Davies R, Nassim MA, Guy MJ, Coupe J, Holgate ST, Moore EA, Bailey AG, and Martonen TB: A technique for simulating radionuclide images from the aerosol deposition pattern in the airway tree. J Aerosol Med. 1997;10:199–212.
9. Fleming JS, Sauret V, Conway JH, Holgate ST, Bailey AG, and Martonen TB: Evaluation of the accuracy and precision of lung aerosol deposition measurements from SPECT using simulation. J Aerosol Med. 2000:13;187–198.
10. Dempster A, Laird N, and Rubin D: Maximum likelihood from incomplete data via the EM algorithm. J R Stat Soc. 1977;39:1–38.

11. Tossici Bolt L, Fleming JS, Conway JH, and Martonen TB: Analytical technique to recover the third dimension in planar imaging of inhaled aerosols: (1) impact on spatial quantification J Aerosol Med. 2000;19:565–579.
12. Fleming JS, Conway JH, Holgate ST, Moore EA, Hashish AH, Bailey AG, and Martonen TB: Evaluation of the accuracy and precision of lung aerosol deposition measurements from planar imaging using simulation. Phys Med Biol. 1998;43:2423–2429.
13. Fleming JS, Sauret V, Conway JH, Martonen TB: Validation of the conceptual anatomical model of the lung airway. J Aerosol Med. 2004;17:260–269.
14. ICRP Publication 66: *Human Respiratory Tract Model for Radiological Protection. 1994 International Commission for Radiological Protection*. Oxford: Pergamon Press; 1994.
15. Weibel ER: *Morphometry of the Human Lung.* Heidelberg: Springer Verlag; 1963.
16. Moller W, Felten K, Meyer G, Meyer P, Seitz J, and Kreyling WG: Corrections in dose assessment of Tc-99m radiolabeled aerosol particles targeted to central human airways using planar gamma camera imaging J Aerosol Med Pulmon Drug Del. 2009;22:45–54.
17. Lee Z, Berridge MS, Nelson AD, and Heald DL: The effect of scatter and attenuation on aerosol deposition as determined by gamma scintigraphy. J Aerosol Med. 2001;14:167–183.
18. Pitcairn GR, and Newman SP: Tissue attenuation corrections in gamma scintigraphy. J Aerosol Med. 1997;10:187–198.
19. Fleming JS Conway JH, and Tossici-Bolt L: Determining regional attenuation correction values for planar scintigraphy using CT images of the thorax. J Aerosol Med Pulmon Drug Del. 2009;22:182.
20. Fleming JS, Epps B, Conway JH, and Martonen TB: Comparison of SPECT aerosol deposition data with a human respiratory tract model. J Aerosol Med. 2006;19:268–278.
21. Fleming JS, Quint M, Bolt L, Martonen TB, and Conway JH: Comparison of SPECT aerosol deposition data with twenty-four hour clearance measurements. J Aerosol Med. 2006;19: 261–267.
22. Montesantos S, Fleming JS, and Tossici-Bolt L: A spatial model of the human airway tree: Part 1. The Hybrid Conceptual Model. J Aerosol Med Pulmon Drug Del. 2010;23:59–68.
23. Schroeter JD, Fleming, JS Hwang D, and Martonen TB: A computer model of lung morphology to analyze SPECT images. Comput Med Imaging Graph 2002;26:237–246.
24. Kitaoka H, Takaki R, and Suki B: A three-dimensional model of the human airway tree. J Appl Physiol. 1999;87:2207–2217.
25. Tawhai MH, Pullan AJ, and Hunter PJ: Generation of an anatomically based 3D model of the conducting airways. Ann Biomed Eng. 2000;28:793–802.
26. Bennett WD, Brown JS, Zeman KL, Hu S-C, Scheuch G, and Sommerer K: Targeted delivery of aerosols to different lung regions. J Aerosol Med. 2002;15:179–188.
27. Moller W, Meyer G, Scheuch G, Kreyling WG, and Bennett WD: Left-to-right asymmetry of aerosol deposition after shallow bolus inhalation depends on lung ventilation. J Aerosol Med Pulmon Drug Del. 2009;22:333–339.
28. Phipps PR, Gonda I, Bailey DL, Borham P, Bautovich G, and Anderson SD: Comparison of planar and tomographic scintigraphy to measure the penetration index of inhaled aerosols. Am Rev Respir Dis. 1989;139:1516–1523.

Received on July 2, 2010
in final form, September 3, 2010

Reviewed by:
Andy Clark
Steve Newman

Address correspondence to:
John S. Fleming, Ph.D.
Department of Nuclear Medicine
Southampton General Hospital
Southhampton, SO16 6YD, UK

E-mail: john.fleming@suht.swest.nhs.uk